

Elizabeth M. C. Hillman¹, A. J. De Crespigny¹, H. E. D'Arceuil¹, J. B. Mandeville¹, J. J. Marota¹, I. C. Teng², Anders M. Dale³, David A. Boas¹ and Anna Devor^{1,2}

¹Martinos Center for Biomedical Imaging, MGH, Harvard Medical School, Charlestown, MA, ²Department of Neurosciences and ³Departments of Neurosciences Radiology, University of California, San Diego, CA

Introduction

Functional magnetic resonance imaging (fMRI) using blood oxygenation level-dependent (BOLD) contrast is a highly promising technique for non-invasive study of brain activity. However, a number of factors limit the usefulness of the existing fMRI data, and may even result in erroneous conclusions. Interpretation of BOLD contrast in quantitative hemodynamic terms is still under debate. According to existing models BOLD contrast is a complex signal that arises from magnetic disturbances caused by deoxyhemoglobin (Hb) and is derived from both changes in local oxygen metabolism and blood flow [1-3]. In contrast to BOLD, optical methods provide direct and quantitative measures of hemoglobin oxygenation and blood flow. In addition, optical measurements are fully compatible with fMRI [4-6]. We combined quantitative optical imaging of hemodynamic signals directly with concurrent BOLD fMRI in the rat somatosensory cortex aiming to quantitatively characterize BOLD contrast during stimulus-evoked hemodynamic response.

1. Boston, R.B., E.C. Wong, and L.R. Frank. *Dynamics of blood flow and oxygenation changes during brain activation: the balloon model*. Magn Reson Med. 1998; 39(6): p. 855-64.
2. Hoge, R.D., et al. *Investigation of BOLD signal dependence on cerebral blood flow and oxygen consumption: the deoxyhemoglobin dilution model*. Magn Reson Med. 1999; 42(5): p. 849-63.
3. Mandeville, J.B., et al. *Evidence of a cerebrovascular postarteriole windkessel with delayed compliance*. J Cereb Blood Flow Metab. 1999; 19(6): p. 679-89.
4. Kemner, A.J., et al. *Concurrent fMRI and optical measures for the investigation of the hemodynamic response*. Magn Reson Med. 2005; 54(2): p. 354-65.
5. Hoge, R.D., et al. *Simultaneous recording of task-induced changes in blood oxygenation, volume, and flow using diffuse optical imaging and arterial spin-labeling MRI*. Neuroimage. 2005; 25(3): p. 701-7.
6. Huppert, T.J., et al. *A temporal comparison of BOLD, ASL, and NIRS hemodynamic responses to motor stimuli in adult humans*. Neuroimage. 2006; 29(2): p. 368-82.

Methods - MRI

Rats were anesthetized by continuous intravenous infusion of α -chloralose at 40 mg \cdot kg $^{-1}$ \cdot h $^{-1}$. An area of skull overlying SI cortex was exposed and thinned until translucent. A small surface radiofrequency (RF) MRI coil was positioned in a direct contact with the skull encompassing the thinned area. The coil also served as a base for the optical well. The well was built using RTV silicon glue, filled with MR-compatible inert liquid formblin and covered with a plastic or glass cover slip to improve the transparency of the bone tissue and to eliminate surface reflection.

MRI was performed using 4.7T/33cm bore Oxford magnet interfaced to a Bruker Biospec Avance console equipped with 12cm i.d., 380mT/m gradients. The coil was matched and tuned. Coronal pilot images were acquired to determine the slice position for the somatosensory cortex. Global field inhomogeneity was reduced by shimming on the signal from the slices of interest. Subsequent activation experiments were performed with a multi-slice single-shot gradient-recalled echo planar sequence (GRE-EPI). The following parameters were used: FOV 19.2 mm 2 ; 75 $^\circ$ flip angle; 600 μ m slice thickness; 64x64 matrix size; 300x300 mm in-plane resolution; TR/TE=500/35 msec; n=5 slices, rostral-caudal readout direction. The slices were acquired either in coronal or oblique orientation. Oblique slices were positioned to cut tangentially through the somatosensory cortex (to match the optical imaging plane). Standard phase correction was used to minimize Nyquist ghosting.

Pulsed electrical stimuli were applied to the whisker pad at 1, 1.5 or 2 mA in 10 s blocks with 36 s inter-block interval. Scans were acquired in sessions of 3 min (360 TRs) during 5 repetitions of 10 sec stimulus blocks with 36 sec ISI for block trials. High resolution structural scans were acquired using a conventional gradient echo sequence, voxel size 75x75x300 mm, TR 500 ms, TE 10 ms.

A "sync" pulse programmed from the MRI scanner was also recorded by the optical imaging system to allow accurate temporal registration of the data.

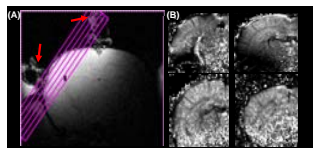


Figure 1. T₂* relaxation maps. Maps of T₂* relaxation time show relatively uniform relaxation up to the edge of the cortex; i.e. minimal artifacts from the thinned skull area. T₂* maps also highlight veins penetrating cortex and also with in deep white matter. A. Oblique slice positioning on coronal localizer image. The edge of the silicone well is also visible (arrows). B. Coronal T₂* maps.

Methods – optical imaging

We have developed an MR-compatible optical imager that uses optical fibers to bring illumination light into the bore of the MRI scanner and a high-density coherent fiber bundle (15000 fibers, Myriad Fibers) to transmit the optical signal to a detector, a cooled CCD camera (Cascade, Roper Scientific). MR-compatible dielectric mirror images a cortical window (thinned bone) onto the coherent fiber bundle that transmits the image to the CCD camera 30 ft away from the MRI scanner. The end of the fiber bundle with the mirror is mounted on a plastic plate. The plate is used to secure the bundle to the animal holder and allows fine positioning. The positioning mechanism secures the mirror-coupled end of the bundle ~1/2" above the animal head. The other end of the bundle is equipped with a lens that allows focusing and zoom and is coupled to the CCD camera. The signal from the high-density coherent bundle is imaged onto the detector using the focusing lens. A non-coherent illumination fiber bundle attached to tungsten-halogen light source is used for illumination. Illuminating light is directed through a dual-position filter switch that alternates between 580 and 610 nm 30 nm-bandpass filters. The filter switch operates at 8 Hz, and provides a trigger signal for the camera at each filter position. Quantitative estimates of the concentrations of Hb, HbO, and HbT are obtained by fitting the observed signal changes at two wavelengths to a model taking into account the respective absorption spectra of HbO and Hb and differential pathlengths.

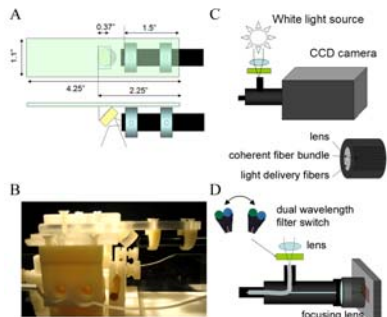


Figure 2. MR-compatible optical imager. A. The distal end of the fiber bundle is coupled to a mirror (yellow). B. A photograph of the distal end mounted onto the animal holder. C-D. At the proximal end the imaging fibers in the bundle are coupled to a CCD detector. Light from the light source is passed through a dual wavelength filter switch and focused onto illuminating fibers.

Standard correlation fMRI maps

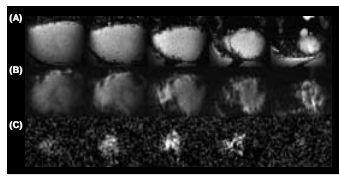


Figure 3. Functional correlation maps. Structural scans (A), single shot EPI (B) and correlation maps (C). Superficial veins are apparent in the structural scans which can form "fiducials" to aid spatial registration with optical images. Localized signal loss in the EPI images are likely due to larger surface veins. Nevertheless, focal areas of activation to whisker pad stimulation are clearly seen. (A) High resolution oblique GRE images. (B) single-shot GRE-EPI images. (C) Standard correlation maps from one stimulation run (5 stimulus repetitions).

Coregistration of optical and MRI images

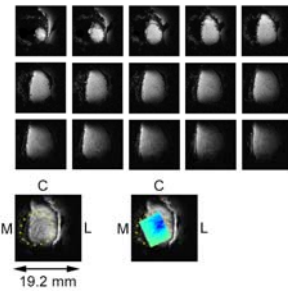


Figure 4. Reconstruction of cortical surface. Cortical surface is reconstructed from oblique structural MRI images. Superficial veins form "fiducials" to aid spatial registration with optical images. Brain surface with pial vessels was reconstructed using high-resolution structural MRI. Top: raw slices in oblique orientation. The optical well is visible in the first 5 slices. Bottom left: reconstructed surface. The position of the well is shown by yellow stars. Bottom right: the optical field of view (FOV) is superimposed on the reconstructed brain surface. Optical FOV shows a ratio image that was calculated 6-7 sec post-stimulus to emphasize draining veins (blue). M – medial, L – lateral, R – rostral, C – caudal.

Colocalization of optical and MRI functional maps

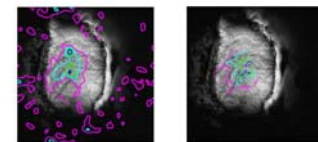
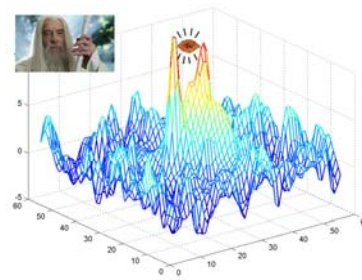


Figure 5. Comparison of BOLD and Hb functional maps. Contours of 0.8, 0.6, 0.4 and 0.2*max of BOLD (left) and Hb (right) superimposed on MRI surface reconstruction.

Conclusions

- Comparison of the timecourse of BOLD fMRI recorded from the brain surface layers and optical measurements demonstrate contribution of both Hb and blood volume. Short TR (500msec), small surface transmit coil (7mm diameter) and high field (4.7T) increase contribution of T1 to the BOLD signal resulting in increased "in flow effects".
- BOLD signal from the brain surface is delayed comparing to deeper layers. This might correspond to delayed activation of pial veins.
- There is close to linear correspondence between the amplitude of BOLD and optical measures on a trial-to-trial basis. This might indicate that trial-to-trial variability reflects fluctuations in cortical (neuronal) responsiveness.



Comparison of spatial maps across stimulus amplitudes

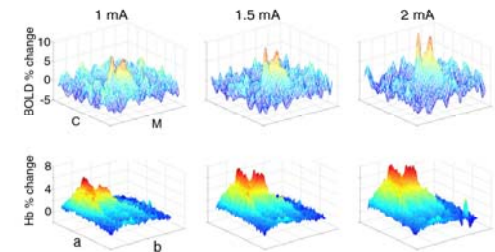


Figure 6. Parametric surfaces of BOLD and Hb responses. Parametric surfaces of BOLD and Hb responses at 3 stimulus intensities. Maps were calculated as mean of images 2-5sec following the stimulus onset normalized by the pre-stimulus baseline.

Comparison of timecourses across stimulus amplitudes

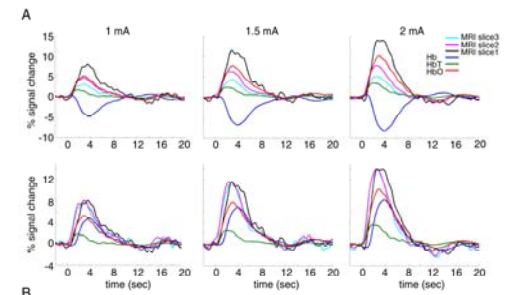


Figure 7. Comparison of functional timecourse of BOLD and optical measures. Timecourses were extracted from ROI within the 0.4*max contour. BOLD response from the brain surface is delayed relative to deeper layers. BOLD surface response peaks earlier than optical measurement of Hb (the same time as HbO). BOLD surface response decay is similar to Hb. Timecourses were extracted from analogous ROIs (~2x2 mm) following spatial coregistration. Three columns correspond to 3 stimulus amplitudes (shown on top). In the second row BOLD timecourses are normalized to the amplitude of the top slice (slice 1), and Hb is inverted for better visualization of differences in response onset time. 20 trials were averaged for each stimulus condition.

Trial-to-trial correlation

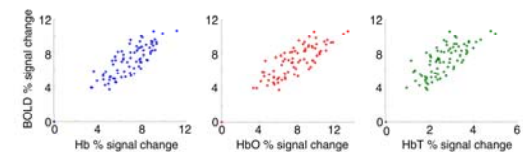


Figure 8. Trial-to-trial correlation of BOLD and optical data. Trial-to-trial comparison of peak response within the same ROI. Each dot represents one trial. All 3 amplitudes are superimposed.

Spontaneous oscillations

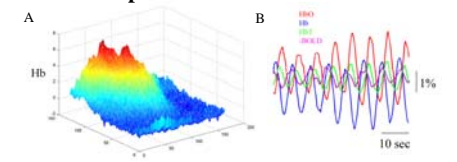


Figure 9. Comparison of BOLD and optical data during spontaneous "vasomotion". Spontaneous oscillations are evident in all measured parameters: Hb, HbO, HbT and BOLD. No stimulus was present. Compare the spatial profile of Hb to Figure 6. A. Parametric surfaces of Hb during spontaneous oscillations calculated as mean of 5 images at the maximum amplitude divided by the mean of 5 images at the minimum. B. Timecourse of spontaneous oscillations in the region inside 0.5*max contour – comparison of Hb, HbO, HbT and BOLD.